2011 8th International Multi-Conference on Systems, Signals & Devices

AN AUTOMATED VESSEL SEGMENTATION OF RETINAL IMAGES USING MULTISCALE VESSELNESS

Mariem Ben Abdallah, Jihene Malek, Karl Krissian, and Rached Tourki

Electronics and Micro-Electronics Laboratory, *Faculty of Sciences of Monastir*,
Monsatir 5000, Tunisia
Grupo de Imagen, Tecnología Médica y Televisión, University of Las Palmas of Gran Canaria,
Las Palmas 35017, Spain
benabdallah_mariem@yahoo.fr, jihenemalek@yahoo.fr, krissian@dis.ulpgc.es

ABSTRACT

The ocular fundus image can provide information on pathological changes caused by local ocular diseases and early signs of certain systemic diseases, such as diabetes and hypertension. Automated analysis and interpretation of fundus images has become a necessary and important diagnostic procedure in ophthalmology. The extraction of blood vessels from retinal images is an important and challenging task in medical analysis and diagnosis. In this paper, we introduce an implementation of the anisotropic diffusion which allows reducing the noise and better preserving small structures like vessels in 2D images. A vessel detection filter, based on a multi-scale vesselness function, is then applied to enhance vascular structures.

Keywords—Ocular fundus image, blood vessels, Flux-based Anisotropic Diffusion, multiscale vesselness

1. INTRODUCTION

The retinal image is acquired with a medical device called fundus camera, consisting in a powerful digital camera with a dedicated optics [20]. Retinal images of humans play an important role in the detection and diagnosis of many eye diseases for ophthalmologists [22]. Therefore, automatic detection of structures in retinal images is necessary, and among them the detection of blood vessels is most important. The information about blood vessels, such as length, width, tortuosity and branching pattern, provides both information on pathological changes and means to grade diseases severity [21]. However, manual detection of blood vessels is much more difficult since the blood vessels in a retinal image are complex and have low contrast. In addition, several retinal images are usually required to diagnose a disease. Hence, manual measurement becomes tedious. As a result, reliable and automatic methods for extracting and measuring the vessels in retinal images are needed. Several works were have been proposed in the detection of 2D complex vessels network, among them, matched filter [7], adaptive local thresholding [33], ridge-based segmentation [12], single-scale Gabor filters[24], and multiscale Gabor filters[8]. In recent years, alternative approaches for automated vessel segmentation employ multiscale detection of curvilinear structures, which is effective in discerning both large and small vessels. In [30, 6, 34], the eigenvector associated with the minimum eigenvalue of the Hessian matrix across all scales was used to estimate the vessel direction at a given pixel. Frangi and al. [4] developed a vesselness filter using the Hessian matrix eigenvalues. In this paper, we propose a multi-scale response to detect linear structures in 2D images. We will use the formulation, which was proposed in 2D and 3D cases in [30], then was developed in 3D in [6, 34, 15], the reduction in the 2D case is based on [5]. Our detection algorithm is dived in two steps. First, we present a flux based anisotropic diffusion method, and apply it to denoise images corrupted by additive Gaussian noise. Then we compute the multi-scale response from responses computed at a discrete set of scales. In the second step, we use a model of the vessels for interpreting the eigenvalues and the eigenvectors of the Hessian matrix. The method was evaluated using the images of two publicly available databases, the DRIVE database [12] and the STARE database [1]. Prior to analysing the images, they are converted to gray scale from the original RGB images.

2. METHODOLOGY

2.1. Techniques for Pre-processing

In order to reduce false detection of the border of the camera's aperture by the vesselness transformation, an iterative algorithm has been proposed by [11]. It aims at is to removing the strong contrast between the retinal fundus and the region outside the aperture (Figure 1).

978-1-4577-0411-6/11/$26.00 ©2011 IEEE

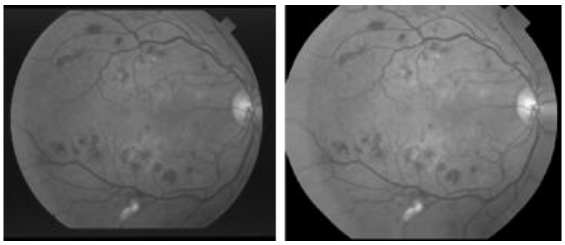

(a) (b)

Figure 1. Fundus image pre-pocessing for removing undesired border effects; (a) Gray-scale of original fundus image; (b) Pre-pocessed image with extended border, (Number of iterations=30).

In the ocular fundus image, edges and local details between heterogeneous regions are the most interesting part for clinicians. Therefore, to preserve and to enhance edges and local fine structures and at the same time reducing the noise is very important. To reduce image noise, several approaches have been proposed using techniques such as linear and nonlinear filtering. In linear spatial filtering such as Gaussian filtering, the content of a pixel is given the value of the weighted average of its immediate neighbors. This filtering reduces the amplitude of noise fluctuations, but also degrades sharp details such as lines or edges, and the resulting images appear blurred and diffused [17]. This undesirable effect can be reduced or avoided by designing nonlinear filters, the most common technique being median filtering. With median filtering, the value of an output pixel is determined by the median of the neighborhood pixels. This filtering retains edges, but results in a loss of resolution by suppressing fine details [14]. Perona and Malik [23] developed the anisotropic diffusion method, a multi-scale smoothing and edge detection scheme, which is a powerful concept in image processing. In order to perform this task we use a well established smoothing technique called Flux-based Anisotropic Diffusion (FBAD) [16]. It produces simplified versions $u(\bar{x},t)$ of the original image $I(\bar{x})$ as solutions of the nonlinear partial differential equation:

$$\begin{cases} u(\bar{x},0) = I \\ \dfrac{\partial u}{\partial t} = div(F) + \beta(I-u) \end{cases} \qquad (1)$$

where β is a data attachment coefficient. Here the diffusion flux F is decomposed in an orthogonal basis, effectively enabling enhancement of contours as well as diffusion along the contours. To this end, we have selected a 2D basis that depicts the gradient vector direction and the direction orthogonal to the gradient vector. The diffusion function associated to each vector of the basis depends on the first order derivative of the intensity in this direction, instead of the traditional norm of the smoothed gradient. For further details the reader is referred to [16].

2.2. Extraction of the local orientations

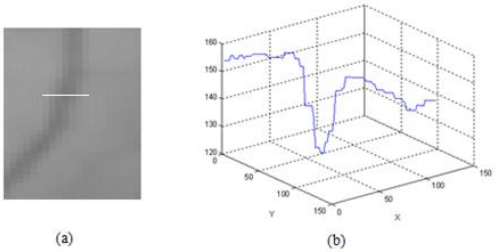

(a) (b)

Figure 2. Example of the cross sectional profile of a blood vessel from a gray scale 2D image. The gray values (intensities) are plotted in a 3D view. The x, y axis is the position of the pixel in the 2D plane of the image, while the z-axis is the gray value or intensity of the pixel.

Our model assumes that the intensity profile of vessels in the cross section is Gaussian (Figure 2). This is a common assumption that is employed in numerous algorithms [31, 4, 19, 1, 15]. It is also commonly assumed that the intensity does not change much along vessels. Although some large vessels in retinal images may have a dark line in their center, such lines can be easily removed by smoothing, and so such lines do not invalidate the Gaussian profile assumption. In recent years, the Hessian matrix can be used to describe the local shape characteristics and orientation for elongated structures [1, 3]. The eigenvalues of this matrix, when the gradient is weak, express the local variation of the intensity in the direction of the associated eigenvectors. Subsequently, we assume that we want to characterize the dark vessels (low intensity) on a white background (high intensity). Let us denote λ_1 and λ_2 the eigenvalues of the Hessian matrix with $\lambda_1 \geq \lambda_2$ and $\vec{v}_1$, $\vec{v}_2$ their associated eigenvectors (Figure 3). For a linear model with Gaussian cross-section, the vessel direction is defined by the eigenvector with smallest eigenvalue at the center of the vessel, but is less determined at the contours because both of the two eigenvalues of the Hessian matrix are zero.

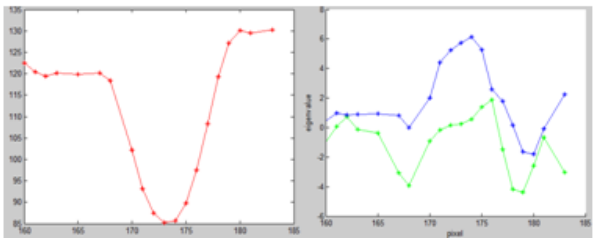

Figure 3. The eigenvalue analysis, left: intensity distribution vessel cross section, right: corresponding eigenvalues; $(\sigma = 4.55)$.

To summarize, for an ideal linear structure in a 2D image:

$$|\lambda_2| \approx 0 \qquad (2)$$

$$|\lambda_1| \succ |\lambda_2| \qquad (3)$$

2.3. Multi-scale image analysis

The idea of multi-scale image analysis is to add a new dimension to the analysis: the – image scale. The image is transformed into a set of derived images, each representing the original image, but at a different scale. While increasing the scale, the image gets progressively blurred and small details are removed. The obtained set is called the scale-space representation of the image. The scale-space theory introduced by Lindeberg uses for the purpose of detail removal a convolution with a Gaussian kernel [32]. Scale-space representation simplifies the contents of the image depending on the chosen scale. It allows to detect objects of similar dimensions as the chosen scale, or to analyze the image across wide range of scales.

2.4. Multi-scale vessel detection

The multi-scale vessel detection is performed for scales between $t_{\min}$ and $t_{\max}$ (corresponding to $\sigma_{\min}$ and $\sigma_{\max}$). For each $\sigma \in \langle \sigma_{\min}; \sigma_{\max} \rangle$, the Hessian matrix entries are calculated. Then the eigenvalue analysis is performed as described in section 2.2 and the result for a given scale is obtained. The final result of the multiscale analysis is the pixel-wise maximum of results obtained over all scales.

2.5. Computation of the multi-scale response

The general approach of multi-scale methods is to choose a range of scales, which are discretized using a logarithmic scale in order to have more accuracy for low scales, and to compute a response for each scale from the initial image. The user specifies the minimal and maximal radius of the vessels to extract. Computation of the single scale response requires different steps. First, a number of points are pre-selected using the eigenvalues of the Hessian matrix. These points are expected to be near a vessel axis. Then, for each pre-selected point, the response is computed at the current scale. The response function uses eigenvectors of the Hessian matrix of the image to define at each point M an orientation $D(\sigma, \bar{x})$ orthogonal to the axis of a potential vessel that goes through M. From this direction, the two points located at equal distance of M in the direction D are noted M_1 and M_2 (Figure 4). The response $R_\sigma(I)$ at M is taken as the maximum among these two points of the absolute value of the first derivative of the intensity in the direction of D.

$$R_\sigma(\bar{x}) = \max\{\nabla_\sigma I(\sigma, \bar{x} + \sigma \cdot d)\cdot(+d), \nabla_\sigma I(\sigma, \bar{x} - \sigma \cdot d)\cdot(-d)\}, \quad (4)$$

where d is the unitary vector of the direction D .i.e. $d = \|\vec{v}_1\|$.

$\nabla_\sigma I$ is the gradient of the image at the scale σ i.e. obtained by convolution with the first derivative of a Gaussian function of standard deviation σ, multiplying the derivatives by σ ensures the scale invariance property and allows comparing responses obtained from different scales. The gradient vector $\nabla_\sigma I$ can be computed by bilinear interpolation for better accuracy, which is especially needed when looking at small vessels.

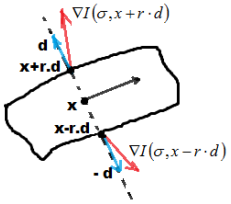

Figure 4. Illustration of the vesselness measure calculation. From the point x on the central line, d is the unit vector perpendicular to the main direction of the vessel and r is the current scale.

For a fixed scale t, we calculate a response image $R_t(I)$ where I is the initial image. Then we calculate the multi-scale response for the image $R_{multi}(I)$ which is the maximum of the responses over scales:
for each point $\bar{x} \in I$ and a range $[t_l, t_h]$ of scale,

$$R_{multi}(\bar{x}) = \max_t \{R_t(\bar{x}), t \in [t_l, t_h]\} \quad (5)$$

This response $R_{multi}(\bar{x})$ can be interpreted as an indicator that the point $\bar{x}$ belongs to the center line of a vessel, and $R_t(\bar{x})$ can be interpreted as an indicator that the point $\bar{x}$ belongs to the center line of a vessel with radius t. Finally, this response is normalized (section 2.6) in order to give a multi-scale response that combines interesting features of each single scale response.

2.6. Normalization

One difficulty with multi-scale approach is that we want to compare the result of a response function at different scales while the intensity and its derivatives are decreasing functions of scale. So far, all considerations were made at a single scale defined by the scale parameter σ. In his work about scale space theory, Lindeberg [28] showed the need for multi-scale analysis to take the varying size of objects into account. He also showed the necessity of normalizing the spatial derivatives between different scales. Thus, the normalized vesselness response is obtained by the product of the normalization term σ^γ and the final vesselness (Equation (6)).

$$R^*(\Sigma, \gamma, \bar{x}) := \max_{\sigma \in \Sigma} \sigma^\gamma \cdot R(\sigma, \bar{x}) = \max_{i=1,\ldots,n} \sigma_i^{\ \gamma} \cdot R(\sigma_i, \bar{x}) \quad (6)$$

The parameter γ can be used to indicate the preference for a particular scale (Figure 5). If set to one, no scale is preferred. Furthermore, the multiscale response is

obtained by selecting the maximum response over a set of different scales between $\sigma_{\min}$ and $\sigma_{\max}$.

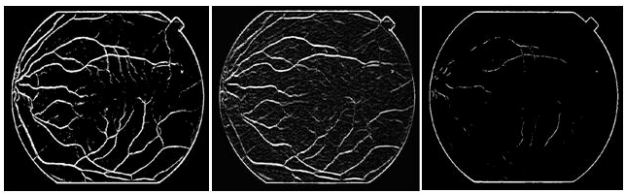

Figure 5. Influence of the normalization parameter γ on the Multi-scale response: Left $\gamma = 1$ is neutral, center $\gamma \succ 1$ favors large scales, finally, right, $\gamma \prec 1$ favors small scales.

3. RESULTS

In this section, experiments have been performed on both synthetic and real retinal images to measure the performance of the proposed enhancement filter in comparison with the standard hand-labeled segmentations, which are manually segmented by two eye specialists. We ran our multi-scale analysis, with the following set of parameters:

- $r_{\min}, r_{\max}, s$, the minimal and maximal radii used in this application are $r_{\min} = 1.25$ and $r_{\max} = 7$, discretized using $s = 4$ scales.
- The parameter γ set to one to indicate no scale is preferred.

Figure 6 presents a result of segmentation with anisotropic scheme. We can see that our filter preserves efficiently the vessels while making the background more homogenous, and improving the contrast.

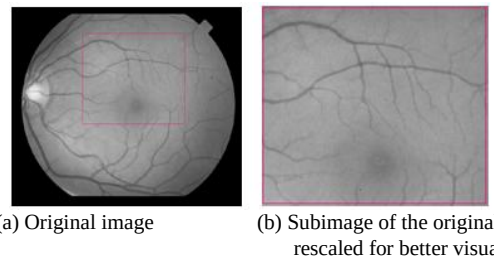

(a) Original image (b) Subimage of the original image, rescaled for better visualization

(c) Segmentation without anisotropic diffusion (d) Segmentation with anisotropic diffusion, $k = 1.25$, $\beta = 0.05$ and $N = 30$

Figure 6. Effect of anisotropic diffusion.

k is a constant threshold.

For computing the response, it is possible to retain the mean of the two calculated values (the gradient of the two points located at equal distance from the current point), like in the 3D case proposed by [15], or a minimum in the 2D case [5]. We preferred to retain a maximum of these two values. As shown in Figure 8 the best response is obtained in the maximum case. The figure shows the results of a synthetic image which was processed by the three filter models.

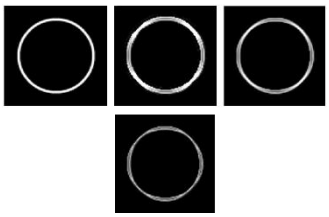

Figure 8. (Left to right- Top to bottom); original image, maximum response, average response, minimum response $\sigma \in \{0.25, 0.5, 1, 2, 4\}$.

Figure 9 shows an example of a medical image from the DRIVE database [12]. The figure also shows that small and large vessels can be distinguished better in maximum case than the minimum or the average cases.

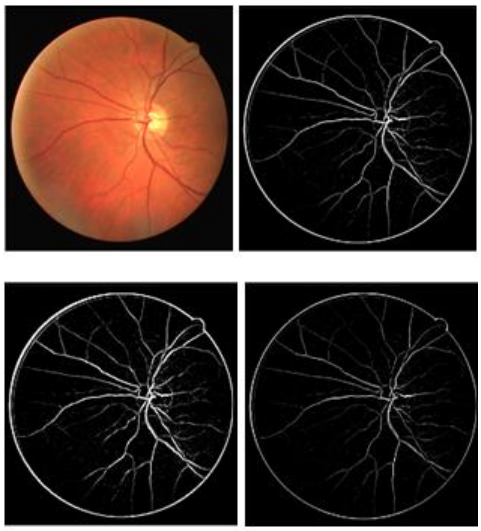

Figure 9. (Left to right- Top to bottom) ; real angiography image [12], average response, maximum response, and minimum response.

We have also applied our method to two-dimensional ocular fundus STARE datasets in order to show the potential of enhancement filtering for improving visualization of the vasculature. Figure 10 Shows Maximum intensity response computed on the original image of Figure 6 (a). Four scales were used for radii of vessels ranging from 1.25 to 7 :{1.25, 2.22, 4, 7}. A vessel of radius r is detected at a scale t, so we use the scales corresponding to each radius for the multi-scale processing.

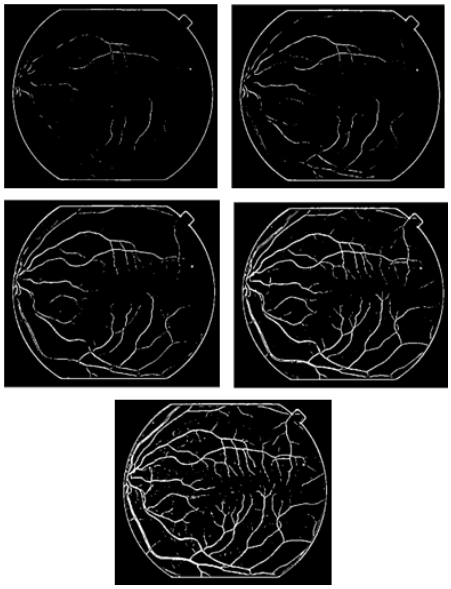

Figure 10. (Top to Bottom) Different responses for different scales; The first four images show the vesselness obtained at increasing scales. The last image is the result after the scale selection procedure.

In Figure 11, an image of the retinal tree vasculature is shown, where performance of subtraction is usually quite good. Although contrast is not very high in Figure 6 (a), the method detects most vessels, over a large size range. Figure 11 demonstrates that it is possible to design a system that approaches the performance of human observers. It can be noticed from these figures that the first and second observer disagree in their manual segmentations. The results presented here demonstrate that our method can produce comparable results to the ground truth, which indicates that the proposed automated method is effective.

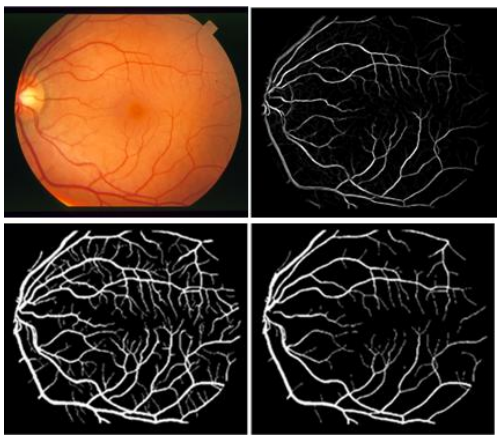

Figure 11. (Left to right- Top to bottom); An image of a retina, the segmented image, and the hand labeled "truth" images (im0077.vk and im0077.ah). [1]

It is common practice to evaluate the performance of retinal vessel segmentation algorithms using ROC curves [12]. A receiver operating characteristic (ROC) curve plots the fraction of pixels correctly classified as vessel, namely the true positive rate (TPR), versus the fraction of pixels wrongly classified as vessel, namely the false positive rate (FPR). The closer the curve approaches the top left corner, the better the performance of the system. The most frequently used performance measure extracted from the ROC curve is the value of the area under the curve (AUC), which is 1 for an ideal system. In the present method, the ROC has been traced by varying the threshold. The curve is shown in Figure 12. The corresponding value of AUC was 0.94514, along with the maximum accuracy (fraction of correctly classified pixel of the automatic and manuel segmentation) corresponding to an "optimum" threshold value (T= 4.000). In the ROC plot, the cut-off point is the closest to [0,1] point or, if you want, the closest to the green line i,e the Cut-off point for best Sensitivity and Specificity (blue circle in plot)= 4.0000.

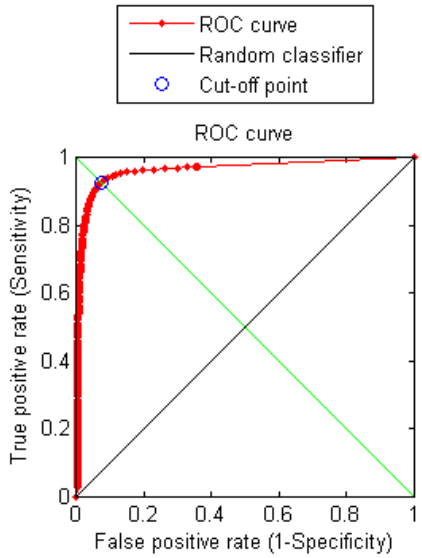

Figure 12. ROC curve for classification on the STARE database using the multiscale vesselness (MM) classifier. The method has AUC = 0.94514.

4. CONLUSION

The purpose of this work is to detect linear structures in 2D retinal images in order to help the interpretation of the vascular network. We proposed to combine an anisotropic diffusion filter to reduce the image noise with a multi-scale response based on the eigenvectors of the Hessian matrix. Our first results show the robustness of the method against noise as well as its applicability to detect blood vessels in 2D retinal images.

5. REFERENCES

[1] A. Hoover, V. Kouznetsova, and M. Goldbaum, "Locating blood vessels in retinal images by piecewise threshold probing of a matched filter response," IEEE Trans. Med. Imag., vol. 19, no. 3, pp. 203–211, Mar. 2000.

[2] A. Can, H. Shen, J.N. Turner , H.L. Tanenbaum, and D. B Roysam, "Rapid automated tracing and feature extraction from retinal fundus images using direct exploratory algorithms,"

IEEE, Transactions on Information Technology in Biomedicine 3(2): pp. 125-138, 1999.
[3] A.P. Witkin, "Scale-space filtering: a new apporach to multi-scale description,"Image Understanding, S. Ullman and W. Richards, Eds, Ablex, Norwood, N.J., pp. 79-95, 1984.
[4] A. Frangi, "Three-dimensional Model-based Analysis of Vascular and Cardiac Images," PhD thesis, Utrecht University, The Netherlands, 2001.
[5] C. Blondel, " Modélisation 3D et 3D+t des artères coronaires à partir de séquences rotationnelles de projections rayons X," PhD thesis, Nice-Sophia Antipolis, pp. 56-86, 29 March 2004.
[6] C. Lorenz, I.-C. Carlsen, T. M. Buzug, C. Fassnacht, J. Weese, Multi- scale line segmentation with automatic estimation of width, contrast and tangential direction in 2d and 3d medical images, in: CVRMed- MRCAS '97: Proceedings of the First Joint Conference on Computer Vision, Virtual Reality and Robotics in Medicine and Medial Robotics and Computer-Assisted Surgery, Springer-Verlag, London, UK, 1997, pp. 233-242.
[7] E. Ardizzone, R. Pirrone, O. Gambino et Francesco Scaturro." Automatic Extraction of Blood Vessels, Bifurcations and End Points in the Retinal Vascular Tree", 13th International Conference on Biomedical Engineering ICBME, 3–6 December, 2008.
[8] F. Oloumi, Rangaraj M. Rangayyan_, Foad Oloumi, Peyman Eshghzadeh- Zanjani, and F´abio J. Ayres; " Detection of Blood Vessels in Fundus Images of the Retina using Gabor Wavelets"; 29th Annual International Conference of the IEEE EMBS ,August 23-26, 2007.
[9] J. Eunhwa Jung, H. Kyungho, "Automatic Retinal Vasculature Structure Tracing and Vascular Landmark Extraction from Human Eye Image," IEEE, International Conference on Hybrid Information Technology (ICHIT'06).
[10] J. Soares, Jorge J.G Leandro, Roberto M. Cesar-Jr., Herbert F. Jelinek, and Michael J. Cree, "Retinal Vessel Segmentation Using the 2-D Morlet Wavelet and supervised Classification" Senior Member; IEEE, May 2006.
[11] J. Staal, M. D. Abramoff, M. Niemeijer, M. A. Viergever, and B. van Ginneken, "Ridge-based vessel segmentation in color images of the retina," IEEE Trans. Med. Imag., vol. 23, no. 4, pp. 501–509, Apr. 2004.
[12] J.J. Koenderink, ++
[13] J S. Lim; 1990 Two-Dimensional Signal and Image Processing (London: Prentice Hall).
[14] K. Krissian, G. Malandain, N. Ayache, R. Vaillant, and Y. Trousset, "Model-based detection of tubular structures in 3D images," Computer Vision and Image Understanding, 80(2): 2000, 130–171.
[15] K. Krissian; " Flux- Based anisotropic Diffusion Applied to enhancement of 3D Angiograms"; IEEE Transactions on Medical Imaging, Vol. 21, No.11.Nov 2002.
[16] K. Murase, M. Ishine, M. Kawamura, S. Tanada, A. Iio and K. Hamamoto 1989 A unified design algorithm of twodimensional digital filters for radioisotope image processing Phys. Med. Biol. 34 859–73
[17] L. Gang, O. Chutatape, and S. M. Krishnan, "Detection and measurement of retinal vessels in fundus images using amplitude modified second-order Gaussian," IEEE Transactions on Biomedical Engineering, 49(2):pp. 168–172, February 2002.
[18] M. Xu and D. Pycock, "A scale-space medialness transform based on boundary concordance voting," Journal of Mathematical Imaging and Vision, 11:277–299, 1999.
[19] M. Sofka and C. V. Stewar, "Retinal vessel extraction using multiscale matched filters confidence and edge measures," Technical Report, the Department of Computer Science, Rensselaer Polytechnic Institute, pp. 05-20, August 16, 2005.
[20] M. A. Rawi, M. Qutaishat and M. Arrar (2007). An improved matched filter for blood vessel detection of digital retinal images, Computers in Biology and Medicine 37(2): 262–267.
[21] N. Patton, T. M. Aslam, T. MacGillivray, I. J. Dearye, B. Dhillon, R. H. Eikelboom, K. Yogesan, and I. J. Constable. "Retinal image analysis: Concepts, applications and potential," Progress in Retinal and Eye Research, 25:99–127, 2006.
[22] P. Perona , J. Malik, .Scale space and edge detection using anisotropic diffusion., IEEE Trans. Pattern Anal. Machine Intell., Vol. 12, pp. 629-639, July 1990.
[23] R.M. Rangayyan,F. Oloumi, F. Oloumi, Eshghzadeh-Zanjani P, and Ayres FJ; "Detection of blood vessels in the retina using Gabor filters" ; dans Proceedings of the 20th Canadian Conference on Electrical and Computer Engineering (CCECE 2007), Vancouver, BC, Canada, April 2007, pages: 22-26. IEEE.
[24] T. Pock, C. Janko, R. Beichel and H. Bischof; " Multiscale Medialness for Robust Segmentation of 3D Tubular Structures"; The Austrian Science Fund (FWF) under the grants P17066-N04. Appeared in:10th Computer Vision with Workshop. February 2005.
[25] T. Chanwimaluang. and G. Fan, "An efficient blood vessel detection algorithm for retinal images using local entropy thresholding,", IEEE International Symposium on Circuits and Systems, Bangkok, Thailand, Vol. 5, pp. 21–24, 2003.
[26] T. Lindeberg and B.M. ter Haar Romeny," Linear scale-space," in Geometry-Driven Diffusion in Computer Vision, B.M. ter Haar Romeny, Ed., Computational Imaging and Vision, pp. 1-72. Kluwer Academic Publishers, Dordrecht, 1994.
[27] T. Lindeberg, "Scale-space theory: A framework for handling image structures at multiple scales," CERN School of Computing, Sep, Egmond aan Zee, the Netherlands, pp. 821, 1996.
[28] T. Lindeberg and D. Fagerstrom, "Scale-space with casual time direction," In ECCV (1), pp. 229–240, 1996.
[29] T. Koller, G. Gerig, G. Székely, and D. Dettwiler, "Multiscale detection of curvilinear structures in 2d and 3d image data," In Fifth International Conference on Computer Vision, Cambridge USA, pp. 864–869, June 1995.
[30] W. Huang, "Automatic detection and quantification of blood vessels in the vicinity of the optic disc in digital retinal images," University of Waikato, 2006.
[31] W. Changhua, G. Agam, P. Stanchev," A general framework for vessel segmentation in retinal images"
[32] X. Jiang and D. Mojon; "Adaptive local thresholding by verification based multithreshold probing with application to vessel detection in retinal images"; IEEE Transactions on Pattern Analysis and Machine Intelligence, 2003, pages:131–137.
[33] Y. Sato, S. Nakajima, N. Shiraga, H. Atsumi, S. Yoshida, T. Koller, G. Gerig, R. Kikinis, Three-dimensional multi-scale line filter for segmentation and visualization of curvilinear structures in medical images, Medical Image Analysis 2 (2) (1998) 143 - 168. doi:DOI: 10.1016/S1361- 8415(98)80009-1.